

EVALUATING THE SURFACE FILM'S PROPERTIES BASED ON ACOUSTIC EMISSION AND CONTACT VOLTAGE SIGNALS

Hiep Xuan Trinh^{1,*}, Tran Van Dua², Ngo Van Quang¹

¹Le Quy Don Technical University, 236 Hoang Quoc Viet, Cau Giay, Ha Noi, Viet Nam

²HaNoi University of Industry, 298 Cau Dien, Bac Tu Liem, Ha Noi, Viet Nam

*Emails: hieptx@mta.edu.vn

Received: 5 February 2021; Accepted for publication: 25 August 2021

Abstract. Methods of creating hard coating films or lubrication are widely used to improve the surface quality of machine parts by reducing the negative effects of friction and wear, resulting in enhanced operational efficiency and lifespan of the machines. The core of these methods is to create intermediate films on the surface of machine parts, preventing their direct contact. The adhesion properties of the coating films on the substrate and the pressure resistance of the lubricant layer are the most important characteristics of these intermediate films. This paper focused on evaluating those properties based on the data of acoustic emission and electrical contact voltage signal. Frictional experiments based on scratch test and pin-on-flat model were conducted with CrN coating, lubricant samples to obtain some experimental data, including contact pressure, friction force, friction coefficient, acoustic emission, and contact voltage. The experimental and analytical results show that the acoustic emission (AE) and contact voltage (VM) signal are reliable for accurately estimating the surface film properties. The acoustic emission data obtained from scratch tests is an effective way to determine adhesion properties of coating films. Whereas the contact voltage signal is better to reveal the possibility of forming the lubricant film. Specifically, by investigating AE and VM values, the optimal adhesion force of CrN coating on SKD11 steel substrate is determined to be 12.3 N, while with DO oil the extreme pressure is 4.8 MPa.

Keywords: Coating film, tribology, acoustic emission, contact voltage.

Classification numbers: 2.5.2, 2.5.3, 5.1.

1. INTRODUCTION

From a mechanical point of view, machine parts always operate based on the interaction of their surfaces through an intermediate material layer or in direct contact, accompanied by friction and abrasion processes. The operation, efficiency, and durability of machines depend mainly on the behavior of their surface parts. The problems of reducing friction and wear are the decisive factors to improve the performance and lifespan of the machines [1 - 3]. Two commonly used solutions to limit the negative effect of friction and wear on the operation of machine parts are the use of lubrication methods and the improvement of surface properties [4 - 6].

The core of the lubrication methods is to form intermediate films based on the adhesion of a lubricant on the machine part's surfaces. That turns the direct contact of the metal surface into the contact of the lubricating film layers, thereby reducing the friction, abrasion, and protecting the machine part's surfaces. Adhesive film layers are formed by the molecular attraction of the lubricant material and the surface layer of machine parts. The ability of the lubricant layer is assessed by its pressure resistance, i.e. the maximum contact pressure at which the lubricating film is not destroyed and the lubricant remains its ability [7, 8]. Thus, the evaluation of the pressure resistance of lubricant film layers plays a crucial role in the machine's efficient operation.

Meanwhile, many methods were proposed to improve the surface properties of machine parts, such as heat treatment [9] and nitriding technology [10]. Currently, the most widely used method is creating hard coating films with good friction and abrasion properties by modern technologies such as CVD (Chemical Vapor Deposition) [11, 12] or PVD (Physical Vapor Deposition) [13, 14]. Many types of coating material were confirmed to significantly improve the surface quality such as chrome- or titan-based hard coating CrN, TiN, TiAlN [15 - 18]. The adhesion of the coating film on the material substrate is one of the most important properties [19].

The lubricating layer and the protective coating film can be considered as the surface film. Many methods were used to evaluate the properties of surface films. In terms of lubrication, the most popular methods used to assess lubricant properties are the model of ball-on-three-balls [20], pin-on-disc [21], or three-ball-on-disc [22]. In terms of assessing the adhesion ability of the coating films, there are several widely used methods such as the pull-off test [23], the sandwich specimen-based method [24], four-point bend specimen [25], indentation test [26], and peel test [27]. Nonetheless, these methods are complex, time-consuming, and complicated to handle for data processing. Therefore, a simple method to intuitively evaluate surface film properties needs to be addressed. In this paper, based on the idea of the interaction process of the machine part's surfaces, besides the appearance of friction and abrasion, there are also other physical phenomena such as contact acoustic emission and contact electrical voltage. The intrinsic of these phenomena is related to the molecular interactions of the surface layers. Thus, they can be used to reflect the contact behavior and evaluate the properties of the surface films.

Regarding the use of scratch test to evaluate the adhesion force of the coating film, the authors in [28, 29] conducted scratch experiments with balls and pins. The scratch was then examined with an optical microscope and the adhesion forces were estimated through the first sign of coating chipping. These methods have high requirements on sample preservation conditions and the use of image processing equipment. In this research, we exploited the scratch test with analysis of acoustic emission (AE) to calculate the adhesion force of film coatings on metal substrates. Micro-blades were used in the scratch model, which is the most effective way to evaluate the adhesion properties of hard coating films because with a micro-blade the contact stress is concentrated near the surface film rather than distributed into the substrate as in the case of ball or pin contact geometry. Besides, other experiments of pin-on-flat model with the analysis of acoustic emission and contact voltage data were conducted to assess the extreme pressure of lubricant films.

In Section 2, the methods used in this research are introduced, then Section 3 presents the experimental setup, the results obtained, and the discussion. Finally, our paper is concluded with a description of limitations and future work.

2. METHODS

Contact Acoustic Emission (AE) is a form of high-frequency sound, generated by releasing the energy from a material surface. The intrinsic of the contact acoustic emission is due to the deformation and destruction of the surface layers. The interactions of sliding surfaces result in the deformation, adhesion, and material removal. These processes are the source of contact acoustic emission. Similarly, the contact voltage (VM) results from the displacement of atoms in the molecular interaction of the surface layers. The magnitudes of AE and VM depend on the physical properties of the surface films.

In the scratch test model diagram (Figure 1), the coating sample is placed below and the micro-blade is above. The position sensor (4) and the acoustic sensor (2) are attached to the blade holder (3). The holder has a position sensor to control its vertical motion. The acoustic sensor records the contact acoustic emission as the blade cut into the coating sample. The vertical load F_z applied to the blade is increased linearly, controlled by the force sensor.

The measuring process with the scratch model is as follows: First, the micro-blade contacts the coating sample at point A with the vertical load F_z of P_1 (N), then the blade moves horizontally to point C on the coating sample with the vertical load increasing linearly to the value of P_2 (N). On the AC segment, the blade cut progressively into the coating sample, resulting in material removal of both the coating layer and the substrate. In the AB segment, the cutting mechanism is delaminating, thus the AE signal is smooth with relatively small magnitudes. At point B on the AC segment, the coating film was completely cut through by the micro-blade at the critical load (L_c). At this critical load, the AE signal fluctuated much more strongly, because the micro-blade was in contact with the steel substrate after cutting through the coating. At the same time the detachment of the coating occurs, the incision begins to take the shape of a sawtooth. Thus, the critical load of the coating samples can be calculated by extracting the value of normal force at the corresponding moment of the AE signal. The critical load L_c is the adhesion force that is used to evaluate the adhesion properties of coating film on the substrate surface.

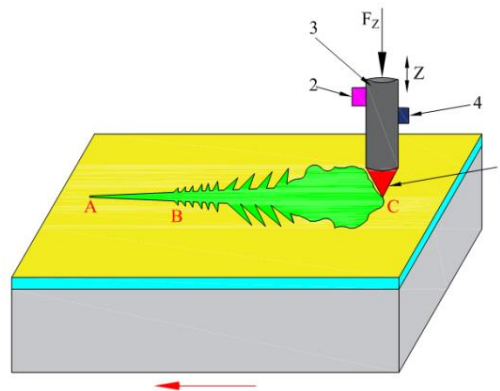


Figure 1. Schematic Model of Scratch Test. (1) Micro-Blade, (2) Acoustic Sensor, (3) Blade holder with Position Sensor (4).

Regarding the extreme pressure (EP) of the lubricant film, the evaluating diagram with the pin-on-flat model is depicted in Figure 2. In this model, the pin and flat are made of metal, and the flat has a layer of lubricant on the surface. The acoustic sensor and electrical sensor are used to measure the magnitude of AE and VM. The pin is in contact with the flat at a linearly increasing vertical load, and the flat motion is reciprocating. First, at a small vertical load, the pin contacts the flat through the lubricant film. At this stage, the AE signal is smooth with a small magnitude. Also, due to the electrical isolation characteristic of the lubricating film, the

value of the electrical resistance is high, thus the magnitude of VM in this period is maximum. Then at extreme pressure, the lubricating film is cut through, the pin is in direct contact with the flat, resulting in a significant increase and strong fluctuation of AE. The magnitude of VM signal also decreases sharply. Thus, by assessing the data output of AE and VM signals, the pressure resistance of lubricant can be estimated.

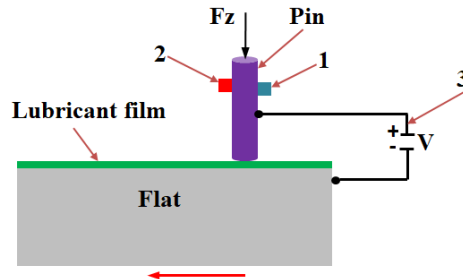


Figure 2. Schematic model of pin-on-flat test; (1) Position Sensor, (2) Acoustic Sensor, (3) Voltage Sensor.

3. EXPERIMENTS AND DISCUSSION

3.1. Evaluating adhesion properties of the coating film

In this research, to verify the effectiveness of the method used to evaluate the adhesion properties of the coating films by exploiting the acoustic emission signal, we used samples with CrN coating on the SKD11 steel substrate by PVD sputtering technology. The composition of SKD11 steel is given in Table 1. Chromium and nitrite target with 99.99 % purity was used in this coating process, whose parameters are summarized in Table 2. Some parameters including sample temperature, rate of nitrogen, and DC pulse frequency were controlled to show their influences on the adhesion of the CrN coating film. The coating samples are shown in Figure 3.

Table 1. Chemical deposition of steel SKD11

C (%)	Si (%)	Mn (%)	Cr (%)	Mo (%)	V (%)	P (%)	S (%)
1.4	0.5	0.39	11.24	0.83	0.205	<0.017	<0.0005

Table 2. Parameters of the CrN coating process

Parameters	Value
Pressure chamber, Pa	8×10^{-2}
Distance from substrate carrier to target	100 mm
Argon rate	12 sccm
Dc pulse frequency (A)	50 to 150 kHz
Nitrogen rate (B)	4 to 8 sccm
Sample temperature (C)	100 °C to 300 °C
Coating duration	90 minutes



Figure 3. Specimens with CrN coating on SKD11 steel.

The adhesion properties of the coating specimens were evaluated by using scratch tests conducted on a Universal Micro Material tester (UMT) system (CETR-USA)¹. The experimental setup is shown in Figure 4. The CrN coating sample is the lower specimen and is attached to a horizontal reciprocating linear motion that can provide a linear movement with various velocity magnitudes. The upper specimen is a diamond blade attached to the spring suspension through an adapter. The suspension was directly connected to the 2D force sensor for measuring vertical force (F_z) and horizontal force (F_x) with a range of 0.2 N to 20 N and 1 mN resolution. The force sensor was placed on the mounting block and was connected to a vertical linear motion system that provided the precise movement with a $5 \cdot 10^{-5}$ mm position resolution. The 2D force sensor provides feedback to control the diamond blade's position to vary the vertical force as in the testing script and automatically measures the value of friction force. In this experimental setup, the Contact Acoustic Emission (AE) sensor with a frequency response of 0.2 to 5 MHz was also used to evaluate the coating film's behavior during the scratch testing process. The experiments were conducted on a fully automated PC-based motor-control system and a data acquisition software, so the testing data can be acquired, calculated, displayed in real-time, and stored. The scratch testing parameters are summarized in Table 3.

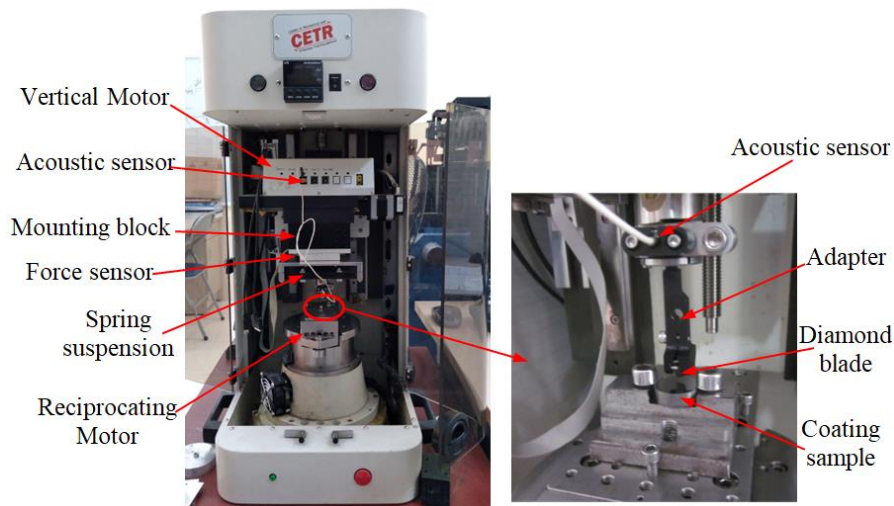


Figure 4. Scratch testing model

¹<https://www.bruker.com/products/surface-and-dimensionalanalysis/tribometers-and-mechanical-testers/umt-tribolab/overview.html>

Table 3. Scratch testing parameters

Vertical load	Scratch testing duration	Scratch length
0N to 14N	20 seconds	5 mm

Figures 5, 6, 7 show the scratch testing results of some coating specimens. In these figures the vertical load (Fz) is dashed blue, the friction force (Fx) is black, and the acoustic emission (AE) is red. These channels are plotted as a function of testing time within 20 seconds. The normal force (Fz) increased linearly from 0 to 14 N. The PVD coating was completely cut through by the micro-blade at the critical load (Lc). After cutting through the coating, the micro-blade contacted directly the steel substrate, the detachment of the coating occurred, the incision began to take the shape of a sawtooth, and the contact area increased unstably (as depicted in Figure 1). Thus, the friction force was shifted to a higher value with a different slope and it was unstable as well as the AE signal fluctuated much more strongly. The critical load of the coating samples can be calculated by extracting the value of normal force at the corresponding moment of the AE signal. (In Figures 5, 6, 7 the corresponding moment of critical load and its values are marked by a black vertical dot line and black arrow).

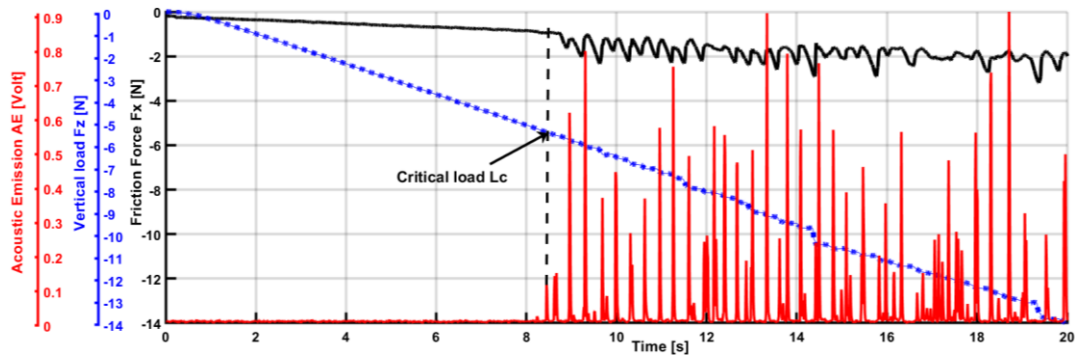


Figure 5. Scratch testing result shows the critical load $L_c = 7.2$ N of the CrN coating sample with coating parameters $A = 50$ kHz, $B = 4$ sccm, $C = 200$ °C

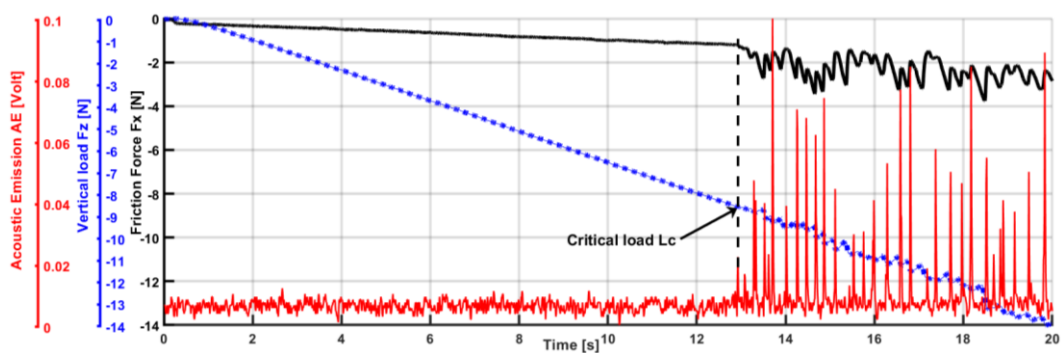


Figure 6. Scratch testing result shows the critical load $L_c = 9.5$ N of the CrN coating sample with coating parameters $A = 100$ kHz, $B = 4$ sccm, $C = 100$ °C

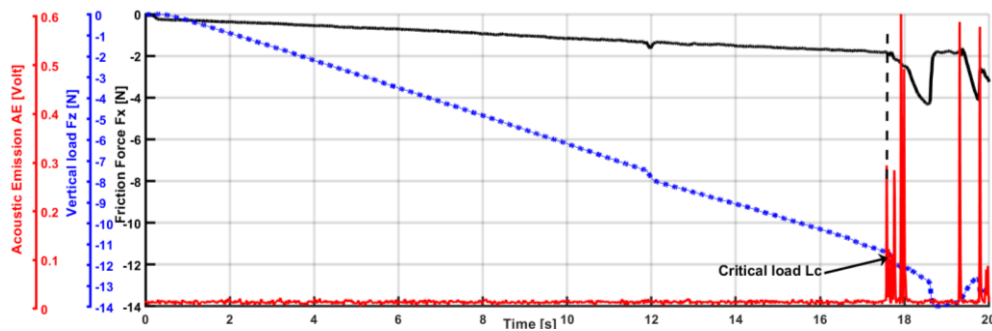


Figure 7. Scratch testing result shows the critical load $L_c = 12.3$ N of the CrN coating sample with coating parameters $A = 100$ kHz, $B = 8$ sccm, $C = 300$ °C

The difference in adhesion force of these coating specimens also indicates the effect of coating parameters on the properties of the formed coating film. Thus, scratch testing with the analysis of the acoustic emission data obtained is an effective way to determine the coating parameters for optimal adhesion properties. Based on the scratch testing results of all coating samples, we find the DC pulse sputtering parameters to optimize the adhesion force of CrN coating to the SKD11 steel substrate. These parameters are $A = 100$ kHz, $B = 8$ sccm, $C = 300$ °C and the optimal adhesion force is 12.3 N. This value is similar to that in the previous research [30].

3.2. Evaluating properties of the lubricant film layer

The experiment is conducted based on the pin-on-flat model as in Figure 8. The experimental setup is similar to the model used in the scratch tests. In the pin-on-flat experiment, the pin and the flat are made of steel 1X18H9T and steel X12M, respectively. The compositions of steel 1X18H9T and X12M are shown in Tables 4, 5. To investigate the properties of lubricant film, we used both the AE sensor and VM sensor. One pole of the VM sensor is attached to the upper sample (pin) and the other pole to the flat. The vertical load increases linearly from 2 N to 120 N. The size of the cylindrical pin is $\Phi 4.6 \times 20$ mm, the corresponding stress can be calculated as follows: Corresponding stress = vertical load/cross-sectional area of the pin.



Figure 8. Evaluating properties of lubricating film layer based on the pin-on-flat model.

Table 4. Chemical deposition of steel 1X18H9T

C (%)	Si (%)	Mn (%)	Cr (%)	Mo (%)	V (%)	P (%)	S (%)
1.4	0.275	0.39	11.24	0.83	0.205	<0.017	<0.0005

Table 5. Chemical deposition of steel X12M

C (%)	Si (%)	Mn (%)	Cr (%)	Mo (%)	W (%)	P (%)	S (%)	No	Ti	Ni	V
0.11 - 0.26	0.1 - 0.4	0.15 - 0.45	10 - 13	0.5 - 2	0.5 - 4	< 0.03	< 0.03	< 0.6	< 0.15	< 0.1	< 0.3

Table 6. Experimental conditions of the pin-on-flat model with lubrication.

Velocity	Vertical load	Duration	Temperature	Lubrication
10 mm/s	From 2N to 120N	20 minutes	25 ⁰ C - 30 ⁰ C	Yes

Several lubricant materials were used for comparison. The experimental conditions of the pin-on-flat model are given in Table 6. The experimental result with DO oil is shown in Fig.11

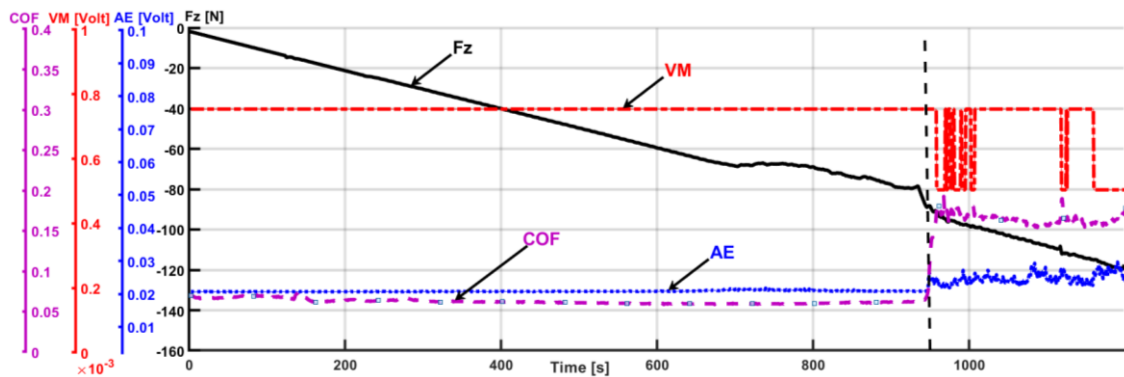


Figure 11. The experimental result with DO lubricating oil.

The experimental result in Figure 11 shows that when the vertical load (F_z) increases from 2 N to 120 N, the frictional process can be divided into two stages with the corresponding behavior of the friction coefficient (COF), acoustic emission (AE), and contact voltage (VM).

In the first stage, the vertical load rises from 2 N to about 80 N (corresponding stress from 0.12 MPa to 4.8 MPa), the friction coefficient is stable with small values. It can be explained that at this stage, the pressure resistance of the DO oil is ensured because the lubricant film still retains a sufficient thickness. So the contact between the pin and flat is indirect through the lubricant film, resulting in the minimum magnitude of AE signal. The results obtained from the contact voltage (VM) also allow to confirm the existence of the lubricating film during this period. Indeed, the contact voltage is stable up to its maximum value due to the good electrical insulating properties of the lubricant layer. Thus, through the investigation of AE and VM values, it can be determined that with DO oil, the ability to form and maintain a protective film of the lubricant is very good at a contact pressure of about 4.8 MPa, or the extreme pressure of DO lubricant is 4.8 MPa. This value is within the extreme pressure range of conventional lubricants, which was observed in [31], using the ball on three ball testing.

The next stage starts at a load of 80 N, which is characterized by a noticeable increase of friction coefficient, accompanied by a significant decrease in VM values and a sharp increase in AE values. It can be explained that in this stage the lubricant film has been cut through, the pin

contacts directly the flat surface. Due to the good electrical conductivity of the metal, the electrical contact resistance is very small, resulting in the negligible value of VM. Thus, the VM and AE signals are reliable data for evaluating the ability of lubricant, as well as calculating its pressure resistance. To clarify strongly this confirmation, two lubricating liquids with higher pressure resistance have been tested under the same testing conditions as for the DO oil. The lubricants are blends of CN20 oil with additive components to improve lubricity and pressure resistance. These compositions are as follows:

- Lubricant 1: CN20 oil with added soap, nano graphite, oleic acid in the ratio 40:20:20:20.
- Lubricant 2: CN20 with added soap, raw graphite, oleic acid in the ratio 40:20:20:20.

The experimental results for the above lubricants are shown in Figures 12, 13, 14.

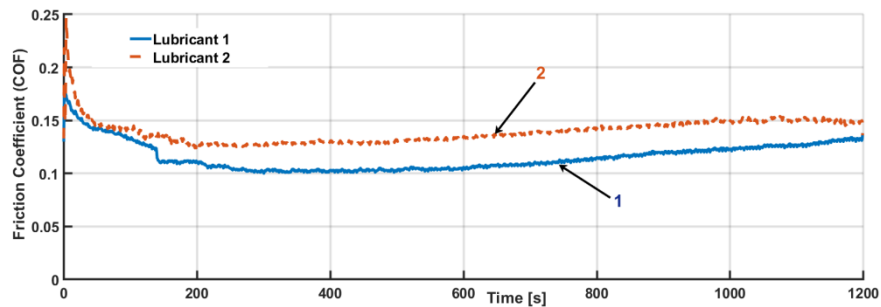


Figure 12. Friction Coefficient (COF) with two lubricants; 1- with lubricant 1, 2- with lubricant 2.

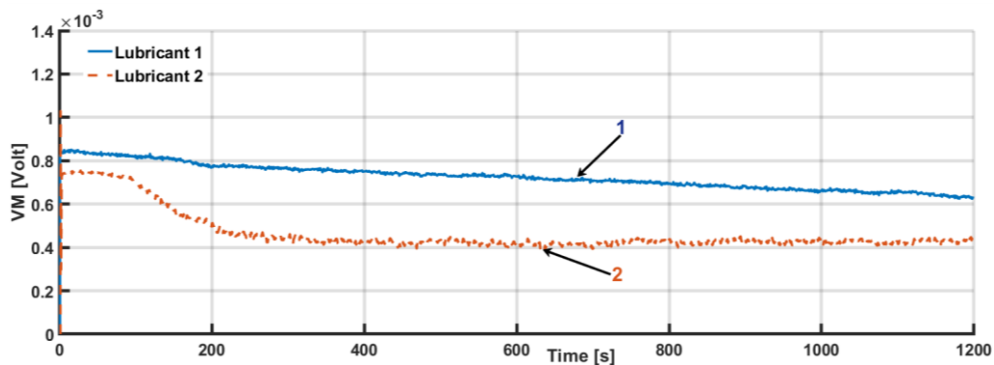


Figure 13. Contact voltage (VM) with two lubricants; 1- with lubricant 1; 2- with lubricant 2.

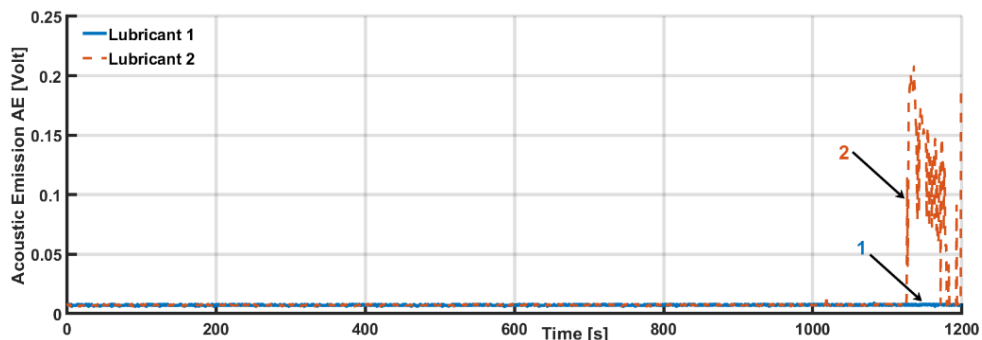


Figure 14. Contact acoustic emission (AE) with two lubricants; 1- with lubricant 1, 2- with lubricant 2.

The average values of friction coefficient, contact voltage, and acoustic emission under the lubricating condition with two lubricants are summarized in Table 8.

Table 8. Experimental results of lubricants 1, 2.

Average value Lubricant	Friction coefficient	Contact Voltage VM (Volt)	Acoustic Emission AE (Volt)
Lubricant 1	0,1289	0,0007568	0.00611
Lubricant 2	0,1397	0.0004527	0.01292

From the experimental results, both lubricants have a good lubrication effect, especially at the high load. The data in Figure 12 and Table 8 show that lubricant 1 has a lower friction coefficient in comparison with lubricant 2, which is also reflected through comparing the contact voltage values. Indeed, the VM value of lubricant 1 is higher than that of lubricant 2, which means the ability to form a protective film of lubricant 1 is better than lubricant 2. Nonetheless, the VM values of both lubricant 1 and lubricant 2 are small (Table 8), which implies that the electrical insulating properties of these lubricants are negligible and the surface-active additive (graphite) does not influence contact voltage. Fig.13 shows that the contact acoustic emission of both lubricants is smooth with very small values. However, with lubricant 2 when the load increases up to about 100 N (corresponding stress of 6 MPa), the AE signal has a strong fluctuation. It can be explained that at that point, the raw graphite particles in lubricant 2 have lost their pressure resistance. The nano graphite particles have better surface protection.

Thus, the contact acoustic emission and contact voltage signals obtained during the frictional interaction under lubricating conditions reflect exactly the lubricant's ability and its pressure resistance. The contact voltage signal is better to reveal the possibility of forming the lubricant film, while the acoustic signal is more sensitive to the change of this film layer.

4. CONCLUSION

In this paper, we used the contact voltage and acoustic emission to evaluate the properties of surface film layers with two cases of study, including the CrN coating and lubricant films. The experiments were conducted through the scratch testing model with micro-cutting and the model of pin-on-flat. By analyzing the relationship between the frictional parameters as well as the values of AE and VM, we confirmed that the AE signal in the scratch tests is the effective factor to calculate the adhesion force of the coating film on the substrate surface. For the CrN coating film, the coating process to optimize the adhesion force is determined with the sputtering parameters such as pulse frequency A of 100 kHz, nitrogen rate B of 8 sccm, and sample temperature C of 300 °C. Also, the ability and the extreme pressure value of the lubricants can be evaluated by investigating the AE and VM signals. The extreme pressure of DO lubricant is estimated with a value of 4.8 MPa. The testing results of the blended CN20 oil lubricants indicate the role of graphite particles to reduce the friction coefficient and improve surface protection. The effect of graphite particles on the value of contact voltage is negligible. The investigation of surface film properties based on the AE and VM signals provides a quick and intuitive assessment. However, in assessing pressure resistance, the influence of some parameters such as the magnitude of velocity or temperature has not been considered. Those problems are the limitation of this research. In the future, we will investigate more thoroughly to improve the efficiency of evaluating the surface film method based on the AE and VM signals.

Author Contributions. Hiep Xuan Trinh: Methodology, data analysis and writing the first draft of the manuscript. Tran Van Dua and Ngo Van Quang: Fabricated experimental samples, conducted experiments and revised the manuscript.

Declaration of competing interest. The authors declare that they have no known competing financial interests or personal relationships that could have appeared to influence the work reported in this paper.

REFERENCES

1. Ludema K. C. - Friction, Wear, Lubrication. CRC Press LLC, 1996.
2. Hsu S., *et al.* - Friction reduction using discrete surface textures: Principle and design, *Journal of Physics D Applied Physics* **47** (33) (2014). 10.1088/0022-3727/47/33/335307.
3. Brinksmeier E., *et al.* - Metalworking fluids—Mechanisms and performance, *CIRP Annals* **64** (2) (2015) 605-628. <https://doi.org/10.1016/j.cirp.2015.05.003>.
4. Abdullah M. A., *et al.* - Reducing Wear and Friction by Means of Lubricants Mixtures, *Procedia Engineering* **68** (2013) 338-344. <https://doi.org/10.1016/j.proeng.2013.12.189>.
5. Ching H. A., *et al.* - Effects of surface coating on reducing friction and wear of orthopaedic implants, *Science and Technology of Advanced Materials* **15** (1) (2014).
6. Hoseini M., *et al.* - Tribological investigation of coatings for artificial joints, *Wear*. **264** (11) (2008) 958-966. <https://doi.org/10.1016/j.wear.2007.07.003>.
7. Davey W. - Extreme pressure lubrication, *Industrial Lubrication and Tribology* **7** (6) (1995) 23-27. <https://doi.org/10.1108/eb052341>.
8. David G., *et al.* - Film Thickness and Friction Relationship in Grease Lubricated Rough Contacts, *Lubricants* **5** (34) (2017).
9. Majeed A., *et al.* - Surface quality improvement by parameters analysis, optimization and heat treatment of AlSi10Mg parts manufactured by SLM additive manufacturing, *International Journal of Lightweight Materials and Manufacture* **2** (4) (2019) 288-295. <https://doi.org/10.1016/j.ijlmm.2019.08.001>.
10. Maldzinski L., Tacikowski J. - ZeroFlow gas nitriding of steels, *Thermochemical Surface Engineering of Steels* (2015) 459-483. <https://doi.org/10.1533/9780857096524.3.459>.
11. Fotovvati B., *et al.* - Reducing Wear and Friction of CVD Diamond Films, *Journal of Manufacturing and Materials Processing* **3** (28) (2019). 10.3390/jmmp3010028.
12. Miki H., *et al.* - Friction properties of partially polished CVD diamond films at different sliding speeds, *Diamond and Related Materials* **24** (2012) 167-170. <https://doi.org/10.1016/j.diamond.2012.01.004>.
13. Bienk E. J., *et al.* - Wear and friction properties of hard PVD coatings, *Surface and Coatings Technology* **76-77** (2) (1995) 475-480. [https://doi.org/10.1016/02578972\(95\)02498-0](https://doi.org/10.1016/02578972(95)02498-0).
14. Fox-Rabinovich G. S., *et al.* - Thin-Film PVD Coating Metamaterials Exhibiting Similarities to Natural Processes under Extreme Tribological Conditions, *Nanomaterials*. 10 1720. 10.3390/nano10091720.
15. Lin J., *et al.* - Tribological behavior of thick CrN coatings deposited by modulated pulsed power magnetron sputtering, *Surface and Coatings Technology Journal* **206** (8-9) 2474-2483. <https://doi.org/10.1016/j.surfcoat.2011.10.053>.

16. Lee J. W. - The mechanical properties evaluation of the CrN coatings deposited by the pulsed DC reactive magnetron sputtering, *Surface and Coatings Technology* **200** (10) (2006) 3330-3335. 10.1016/j.surfcoat.2005.07.047.
17. Gerth J., Wiklund U. - The influence of metallic interlayers on the adhesion of PVD TiN coatings on high-speed steel, *Journal of Wear* **264** (9-10) (2008) 885-92. <https://doi.org/10.1016/j.wear.2006.11.053>.
18. Ozkan D., *et al.* - Tribological Behavior of TiAlN, AlTiN, and AlCrN Coatings at Boundary Lubricating Condition, *Tribology letters* **66** (2018). <https://doi.org/10.1007/s11249-018-1111-1>
19. Zalnezhad E., *et al.* - Optimizing the PVD TiN thin film coating's parameters on aerospace AL7075-T6 alloy for higher coating hardness and adhesion with better tribological properties of the coating surface, *The International Journal of Advanced Manufacturing Technology* **64** (2013) 281-290. 10.1007/s00170-012-4022-6.
20. Românu I. C., *et al.* - A simple solution for evaluation of lubricants anti-wear properties, in *IOP Conf. Series: Materials Science and Engineering* **147** (2016) 012025 doi:10.1088/1757-899X/147/1/012025.
21. Trivedi H. K., Bhatt D. V. - Effect of Lubricating Oil on Tribological behaviour in Pin on Disc. Test. Rig., *Tribology in Industry* **39** (2017) 90-99. 10.24874/ti.2017.39.01.10.
22. Marion M., *et al.* - Wear behavior of PVD-coatings, *Tribology in Industry* **34** (2) (2012) 51-56.
23. Naser A. A., Fahad B. M. - Adhesion test for epoxy reinforcing using waste materials applied on concrete surfaces, *IOP Conf. Series: Materials Science and Engineering* **433** (2018) 012004 doi:10.1088/1757-899X/433/1/012004.
24. Jae Won Kim, *et al.* - A study on fracture characteristic of structural adhesive at bonded specimen made by 3D printer, *Journal of Mechanical Science and Technology* **34** (2020) 3295-3302. <https://doi.org/10.1007/s12206-020-0721-3>
25. Zhenjiang Cui, *et al.* - Benchmarking Four Point Bend Adhesion Testing: The Effect of Test Parameters On Adhesion Energy, *AIP Conference Proceedings*, 2005, pp. 788, 507. <https://doi.org/10.1063/1.2063011>
26. Zhenjiang Cui, *et al.* - A sample preparation method for four point bend adhesion studies, *Journal of Materials Research* **19** (5) 1324-1327. DOI: 10.1557/JMR.2004.0177
27. Zha, *et al.* - Investigation of modelling and stress distribution of a coating/substrate system after an indentation test, *International Journal of Mechanical Sciences* **134** (2017) 1-14.
28. Jinju Chen, Bull S. J. - Approaches to investigate delamination and interfacial toughness in coated systems: an overview, *Journal of Physics D: Applied Physics* **44** (3) (2010).
29. Leyu Lin, *et al.* - Friction and wear of PEEK in continuous sliding and unidirectional scratch tests, *Tribology International* **122** (2018) 108-113.
30. van Essen P., *et al.* - Scratch resistance and wear of CrNx coatings, *Surface & Coatings Technology* **200** (2006) 3496-3502.
31. Lin J., *et al.* - The structure and properties of chomium nitridecoatings deposited using dc, pulsed dc and modulated pulse power magnetron sputtering, *Surface & Coating Technology of Journal* **204** (2010) 2230-2239.
32. Deleanu L., *et al.* - SR EN ISO 20623 - A standard for tribological evaluation of lubricants that may bust innovation, in *IOP Conf. Series: Materials Science and Engineering* **997** (2020) 012008. doi:10.1088/1757-899X/997/1/012008.